Journal of Materials Chemistry A

RSC Publishing

COMMUNICATION

View Article Online
View Journal | View Issue

Freestanding CdS nanotube films as efficient photoanodes for photoelectrochemical cells

Cite this: *J. Mater. Chem. A*, 2013, **1**, 9587

Received 23rd May 2013
Accepted 10th July 2013

DOI: 10.1039/c3ta12034a

www.rsc.org/MaterialsA

Wooseok Kim,[a] Minsu Seol,[a] Heejin Kim,[a] James B. Miller,[b] Andrew J. Gellman[b] and Kijung Yong*[a]

Freestanding CdS nanotube films were synthesized for the first time using ZnO nanorod arrays as a sacrificial template. The CdS nanotube films exhibited excellent photo-anodic activities in a photo-electrochemical (PEC) cell.

Recently, freestanding films have attracted much attention because they are highly useful in the fabrication of various nanodevices.[1] Freestanding films can be used on any substrate without deterioration of their own unique properties. Layer-by-layer (LBL) deposition has been used widely in the synthesis of freestanding films, especially of polymer films with specific physical and mechanical properties.[2] As the demand for photoelectrical devices has increased, the focus of attention has moved recently to freestanding light harvesting films. Although some conjugated polymers have been applied as light harvesting materials in photovoltaics, most of them are made as solution types or nanoparticles to coat on the substrates and hardly made as freestanding films for light harvesting. Semiconductors are appropriate light absorbing materials for fabrication of freestanding films. By using a narrow band gap semiconductor, visible light absorption can be enhanced. However, there has not been much research into semiconducting freestanding films owing to the difficulty of growing semiconductors without substrates, thus most freestanding semiconductor films consist of a freestanding organic/inorganic support with attached semiconductor quantum dots rather than of a composite freestanding film.[3]

In the present study, we have developed a novel synthesis route for the fabrication of a large scale, highly uniform, freestanding CdS nanotube film that uses an array of ZnO nanorods as a sacrificial template. This route requires only simple solution reaction steps and the ZnO nanorod template[4] can be prepared on any surface on which freestanding films can easily be produced. ZnO has a wide band gap of 3.37 eV, whereas CdS has a low band gap of 2.4 eV. CdS can absorb and utilize radiation in the visible light region and thus, it is useful as a sensitizing material in optoelectronic and energy devices. In fact, CdS is one of the most widely used sensitizers in recent solar and photoelectrochemical cells (PECs).[5] Our freestanding CdS film has a nanotube structure, which can be thought of as hollow nanorods with both inner and outer surfaces exposed; its relatively large surface-to-volume ratio is expected to exhibit high catalytic activity.[6]

We have tested the use of our freestanding CdS nanotube films as sensitizers in PECs, and investigated their photoelectrochemical activity. For comparison, planar CdS films were prepared and the photocurrent densities of the CdS nanotubes and the planar CdS films were measured and analyzed.

The fabrication of a freestanding CdS nanotube film requires a series of simple solution-based steps. Fig. 1(a) illustrates a procedure for fabrication of the freestanding CdS nanotube film. Firstly, for the growth of the ZnO nanorod template, a ZnO film was coated onto a Ti (or any other) substrate as a seed layer by using RF magnetron sputtering. Then a ZnO nanorod array was grown on the seed layer with a well-known ammonia-solution hydrothermal method that was described previously.[7] A CdS film was then deposited onto the ZnO nanorods by using successive ionic layer adsorption and reaction (SILAR), which is a layer-by-layer growth method that enables precise control of film thickness by varying the number of SILAR cycles.[8] The ZnO/CdS core/shell nanorod array on the substrate was dipped in aqueous sulfuric acid to etch the ZnO nanorods for 5–10 minutes and then only the self-supporting, freestanding CdS film remained on the substrate.

Fig. 1(b) and (c) present cross-sectional SEM images showing the ZnO/CdS core/shell nanorod structure before and after etching of the ZnO nanorods with aqueous sulfuric acid. Through SILAR of CdS on the ZnO nanorods a uniform and high density ZnO/CdS core/shell nanorod film was produced and the

[a]*Surface Chemistry Laboratory of Electronic Materials, Department of Chemical Engineering, Pohang University of Science and Technology (POSTECH), Pohang 790-784, Korea. E-mail: kyong@postech.ac.kr; Fax: +82-54-279-8298; Tel: +82-54-279-2278*

[b]*Department of Chemical Engineering, Carnegie Mellon University, Pittsburgh, Pennsylvania 15213, USA*

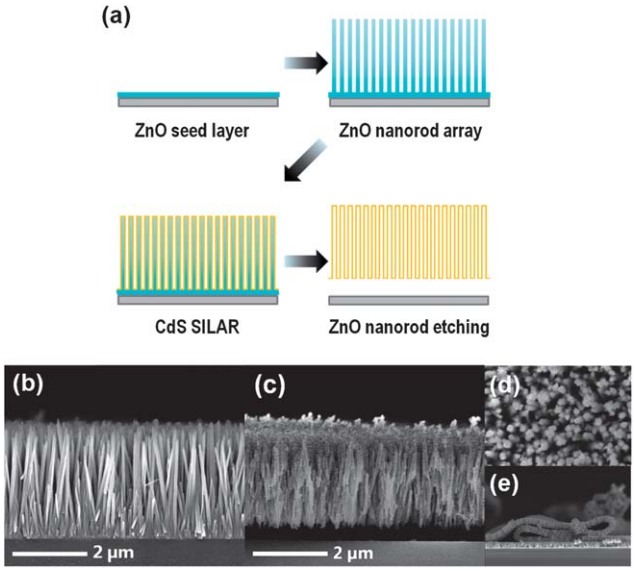

Fig. 1 (a) A schematic diagram showing the procedure for fabrication of a freestanding CdS nanotube film. SEM images of CdS nanotube films (b) before and (c) after the etching of ZnO nanorods. Top view images of CdS nanotubes and folded free-standing CdS nanotube films are shown in (d) and (e), respectively.

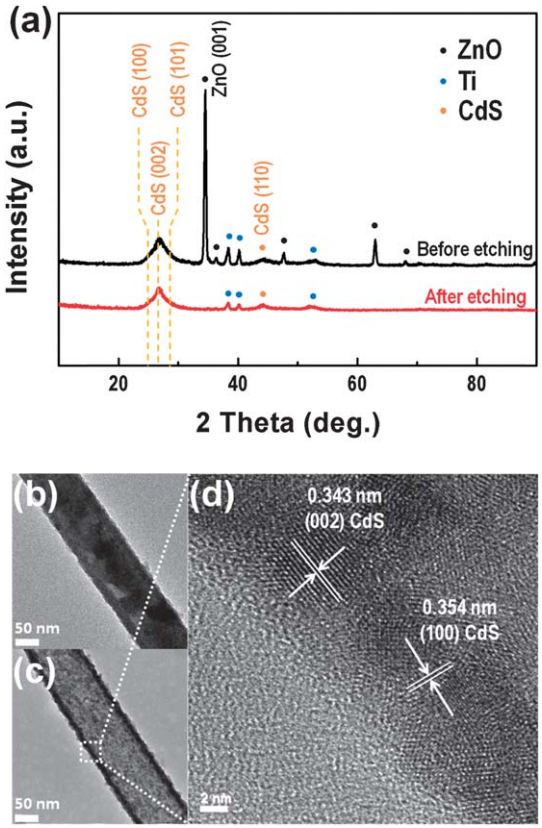

Fig. 2 (a) XRD patterns before and after etching of a ZnO/CdS core/shell structure on a Ti substrate. TEM images of (b) a ZnO/CdS core/shell nanorod and (c) a CdS nanotube and (d) a HRTEM image of the CdS nanotube wall.

thickness of the CdS shell was controlled by the number of SILAR cycles (in this case, 20 cycles of SILAR were used). The CdS-covered ZnO nanorods are approximately 3 μm long and are vertically aligned on the substrate before etching; after etching of the ZnO nanorods, only the CdS nanotube film is freestanding and floating above the substrate. The CdS nanotube film is grown on the ZnO nanorods so its structure is a close-ended configuration as shown in Fig. 1(d). Fig. 1(e) shows a large area freestanding CdS film that can be bent and folded.

The crystal structures of the ZnO/CdS nanorods and CdS nanotubes were confirmed by XRD. In Fig. 2(a), before ZnO etching the three kinds of XRD peaks originate from Ti, CdS, and ZnO, confirming the presence of ZnO/CdS nanorods on the Ti substrate. The CdS peak is rather broad, which indicates that CdS synthesized with SILAR has a polycrystalline structure. The highest peak due to the ZnO nanorods is the (002) peak, which indicates preferential growth of nanorods along the *c*-axis; the other smaller peaks usually originate from the ZnO seed layer. After etching in aqueous sulfuric acid, no ZnO-related peaks are present, which confirms the complete removal of the ZnO nanorod template. The elemental analysis results of EDS (energy dispersive spectroscopy) indicated that the signal intensities of ZnO were negligible after etching reaction. The XRD measurements were performed on freestanding CdS nanotubes on a Ti substrate, so Ti peaks are still present.

To investigate the atomic structure of our CdS nanotube array, HRTEM was used. From the TEM images in Fig. 2(b) and (c), it is evident that the CdS shell has a tubular structure. Fig. 2(d) shows a HRTEM image of the CdS shell after etching. This shell was found to have a uniform thickness of ~10 nm. The polycrystalline CdS shell consists of approximately 5 nm quantum dots with phases of (100) and (002), which is consistent with the XRD results.

The optical absorbance of the CdS nanotube films was examined in the wavelength range 300 to 750 nm. Fig. 3(a) shows that the bare ZnO nanorods (black line) only absorb below 400 nm, which corresponds to the UV region, owing to their wide band gap energy. The CdS nanotube films (red line) absorb over a wider range that includes the UV and visible light regions. The absorption edge values of the bare ZnO nanorods and the CdS nanotube films were found to be 380 nm (3.27 eV) and 530 nm (2.35 eV), respectively.[9] The insets in Fig. 3(a) show freestanding CdS nanotube films on a glass substrate and water. It is transparent and yellow after ZnO etching, whereas before etching the glass was opaque because of the light scattering by the ZnO nanorods.

The CdS nanotube array can be used as a photoelectrode in a PEC hydrogen generation system, because its band gap enables the utilization of the visible region of the incident solar spectrum. Fig. 3(b) shows the current density (I)–potential (V) curves of the CdS nanotube electrode with 1 sun AM1.5G front-side illumination. For comparison, a planar CdS film electrode was fabricated directly on a FTO substrate with the same procedure as used for the CdS nanotube films, and pristine ZnO nanorods were also prepared; the PEC performances of these samples are also included in Fig. 3(b). All measurements were carried out in a three-electrode electrochemical cell with a Pt wire and a saturated calomel electrode as the counter electrode and the reference electrode, respectively. An aqueous solution of 0.25 M

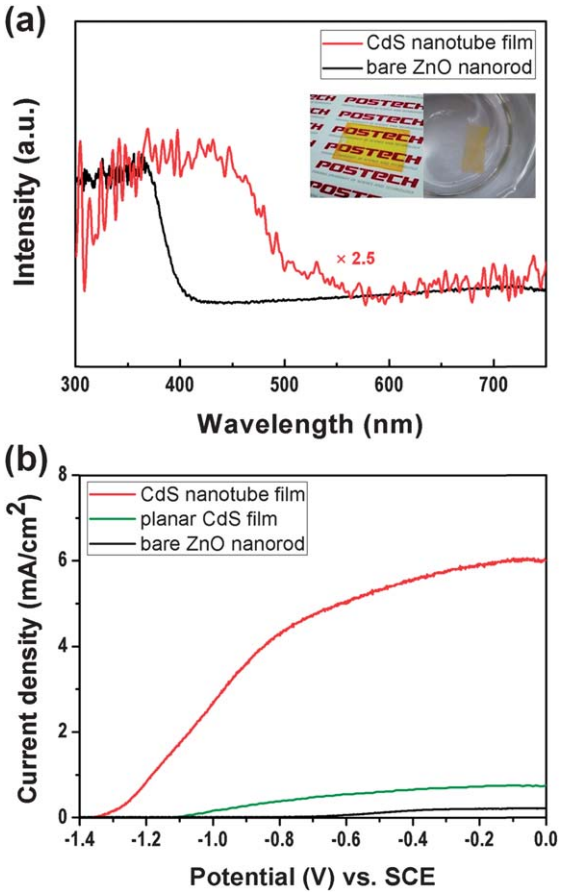

Fig. 3 (a) Diffused reflectance spectra (DRS) of a bare ZnO nanorod array and a freestanding CdS nanotube film. (b) Photocurrent density *vs.* potential curves obtained from PEC cells using various photoanodes; a bare ZnO nanorod array, a planar CdS film, and a CdS nanotube film.

Na_2S and 0.35 M Na_2SO_3 was used as the electrolyte and sacrificial reagent.[10] The pristine ZnO nanorod electrode exhibits an onset potential and a saturation photocurrent density of −0.72 V *vs.* SCE and 0.3 mA cm^{-2}, respectively. The planar CdS film electrode exhibits a more negative onset potential and a higher saturation photocurrent density than the pristine ZnO nanorod electrode, with values of −1.25 V *vs.* SCE and 0.7 mA cm^{-2}, respectively. The more negative onset potential could arise because the position of the quasi-Fermi level of CdS is more negative than that of ZnO. Furthermore, CdS can absorb more photons than ZnO because of its smaller band gap, which means that the photocurrent generation of the planar CdS film is higher. Compared to the planar CdS film electrode, the use of the freestanding CdS nanotubes as an electrode results in a negative shift in the onset potential as well as a substantial improvement in the saturation photocurrent density, with values of −1.34 V *vs.* SCE and 6 mA cm^{-2}, respectively. The larger surface area of the one-dimensional nanotube structure and light trapping through nanotubes explain this great enhancement of the photocurrent density of the CdS nanotube films. Since CdS nanotubes have 1-D structures, the CdS nanotube electrode can absorb far more photons than the planar CdS film electrode due to the light trapping, which induces a high level of photocurrent generation in the CdS nanotube electrode. Moreover, the increased photon absorption and the improved hole transfer to the electrolyte due to the large surface area of the nanotube structure lead to a negative shift in the quasi-Fermi level and thus in the onset potential.[11]

In summary, we have fabricated freestanding CdS nanotube films by using a ZnO nanorod array as a sacrificial template and investigated their structural, optical, and PEC properties. The freestanding CdS films have a polycrystalline tubular structure and exhibit light absorption in the visible light range. As a photoanode in a PEC cell, a CdS nanotube film was found to generate a much higher photocurrent density than a planar CdS film or ZnO nanorods. This result is due to the light trapping and the large surface area of the nanotube structure; hence freestanding CdS films are promising candidates for photoactive layers.

This work was supported by the 2011 Global Research Network Program (220-2011-1-C00033) and NRF Grant (2013R1A2A2A05005344).

Notes and references

1 Y. Sun, Z. Sun, S. Gao, H. Cheng, Q. Liu, J. Piao, T. Yao, C. Wu, S. Hu, S. Wei and Y. Xie, *Nat. Commun.*, 2012, **3**, 1057; D. Feng, Y. Lv, Z. Wu, Y. Dou, L. Han, Z. Sun, Y. Xia, G. Zheng and D. Zhao, *J. Am. Chem. Soc.*, 2011, **133**, 15148; Z. Huang, F. Sun, Y. Zhang, K. Gu, X. Zou, Y. Huang, Q. Wu and Z. Zhang, *J. Colloid Interface Sci.*, 2011, **356**, 783.
2 C. Jiang and V. V. Tsukruk, *Adv. Mater.*, 2006, **18**, 829.
3 Y. H. Liou, L. C. Kao, M. C. Tsai and C. J. Lin, *Electrochem. Commun.*, 2012, **15**, 66.
4 J. J. Wu, W. T. Jiang and W. P. Liao, *Chem. Commun.*, 2010, **46**, 5885; Y. W. Lee, M. A. Lim, S. W. Kang, I. Park and S. W. Han, *Chem. Commun.*, 2011, **47**, 6299.
5 N. D. Sankir and B. Dogan, *J. Mater. Process. Technol.*, 2011, **211**, 382; S. Banerjee, S. K. Mohapatra, P. P. Das and M. Misra, *Chem. Mater.*, 2008, **20**, 6784.
6 G. H. Du, Q. Chen, R. C. Che, Z. Y. Yuan and L. M. Peng, *Appl. Phys. Lett.*, 2001, **79**, 3702.
7 Y. Tak and K. Yong, *J. Phys. Chem. B*, 2005, **109**, 19263.
8 Y. Tak, S. J. Hong, J. S. Lee and K. Yong, *J. Mater. Chem.*, 2009, **19**, 5945.
9 M. Seol, H. Kim, Y. Tak and K. Yong, *Chem. Commun.*, 2010, **46**, 5521.
10 H. Kim, M. Seol, J. Lee and K. Yong, *J. Phys. Chem. C*, 2011, **115**, 25429; S. Cheng, W. Fu, H. Yang, L. Zhang, J. Ma, H. Zhao, M. Sun and L. Yang, *J. Phys. Chem. C*, 2012, **116**, 2615; M. Seol, J. W. Jang, S. Cho, J. S. Lee and K. Yong, *Chem. Mater.*, 2013, **25**, 184.
11 B. Klahr, S. Gimenez, F. Fabregat-Santiago, J. Bisquert and T. W. Hamann, *J. Am. Chem. Soc.*, 2012, **134**, 16693; S. C. Riha, B. M. Klahr, E. C. Tyo, S. Seifert, S. Vajda, M. J. Pellin, T. W. Hamann and A. B. F. Martinson, *ACS Nano*, 2013, **7**, 2396.